Generation of mice with functional inactivation of talpid3, a gene first identified in chicken

Development 138, 3261-3272 (2011) doi:10.1242/dev.063602

Generation of mice with functional inactivation of *talpid3*, a gene first identified in chicken

Fiona Bangs[1], Nicole Antonio[1], Peerapat Thongnuek[1], Monique Welten[1], Megan G. Davey[2], James Briscoe[3] and Cheryll Tickle[1,*]

SUMMARY

Specification of digit number and identity is central to digit pattern in vertebrate limbs. The classical *talpid*^{3} chicken mutant has many unpatterned digits together with defects in other regions, depending on hedgehog (Hh) signalling, and exhibits embryonic lethality. The *talpid*^{3} chicken has a mutation in *KIAA0586*, which encodes a centrosomal protein required for the formation of primary cilia, which are sites of vertebrate Hh signalling. The highly conserved exons 11 and 12 of *KIAA0586* are essential to rescue cilia in *talpid*^{3} chicken mutants. We constitutively deleted these two exons to make a *talpid3*$^{-/-}$ mouse. Mutant mouse embryos lack primary cilia and, like *talpid*^{3} chicken embryos, have face and neural tube defects but also defects in left/right asymmetry. Conditional deletion in mouse limb mesenchyme results in polydactyly and in brachydactyly and a failure of subperisoteal bone formation, defects that are attributable to abnormal sonic hedgehog and Indian hedgehog signalling, respectively. Like *talpid*^{3} chicken limbs, the mutant mouse limbs are syndactylous with uneven digit spacing as reflected in altered *Raldh2* expression, which is normally associated with interdigital mesenchyme. Both mouse and chicken mutant limb buds are broad and short. *talpid3*$^{-/-}$ mouse cells migrate more slowly than wild-type mouse cells, a change in cell behaviour that possibly contributes to altered limb bud morphogenesis. This genetic mouse model will facilitate further conditional approaches, epistatic experiments and open up investigation into the function of the novel *talpid3* gene using the many resources available for mice.

KEY WORDS: Talpid3, Primary cilia, Hedgehog signalling, Limb, Polydactyly, Mouse mutant

INTRODUCTION

Limb development is an outstanding model for investigating pattern formation in vertebrate embryos. Extensive work, mostly on developing chicken wings, has shown that sonic hedgehog (Shh) produced by the polarising region, as discovered by Saunders and Gasseling (Saunders and Gasseling, 1968), at the posterior margin (i.e. that nearer the tail) of the bud is pivotal in digit patterning (Riddle et al., 1993; Yang et al., 1997). The current model for the chicken wing is that Shh diffuses from the polarising region, setting up a concentration gradient across neighbouring cells. Shh modulates the processing of Gli2 and Gli3, which are bifunctional transcriptional effectors of Shh signalling, into transcriptional activators and repressors. High levels of Shh near the polarising region lead to low levels of Gli repressor activity, especially of Gli3, but to high levels of Gli activator activity. Anteriorly, where Shh levels are low, Gli repressors predominate. The ratio of Gli2/3 activator to Gli2/3 repressor is then thought to provide positional information that results in appropriate digits developing in their proper positions (Tickle, 2006). Growth of the field of cells responding to Shh signalling is integrated with patterning to ensure that the correct number of digits form, and Shh signalling has been shown to control the expression of genes encoding cell cycle regulators in the chicken wing bud (Towers et al., 2008).

The classical chicken mutant *talpid*^{3}, in which many morphologically identical digits develop, provides a useful model for exploring digit patterning. The *talpid*^{3} mutation arose spontaneously in a flock (P. Hunton, MSc Thesis, University of London, 1960). Of the other *talpid* chicken mutants with similar phenotypes, the *talpid*^{1} mutant (Cole, 1942) is now extinct; the *talpid*^{2} mutant (Abbott et al., 1959) is maintained in the USA, but it is not known whether it is allelic with *talpid*^{3}. Donald Ede carried out extensive embryological and cellular analyses on the *talpid*^{3} chicken mutant, documenting its abnormalities, in addition to polydactyly, and alterations in cell behaviour (Ede and Kelly, 1964a; Ede and Kelly, 1964b; Ede and Agerbak, 1968). It subsequently emerged that the response to Shh signalling in *talpid*^{3} embryos is abnormal. In *talpid*^{3} wing buds, Shh-responsive 5′ *Hoxd* genes, which are normally posteriorly expressed, are expressed all across the anterior-posterior axis (Izpisúa-Belmonte et al., 1992), whereas the expression of other genes, including *Ptch1* and *Gli1*, is lost (Lewis et al., 1999). Furthermore, the development of all the regions affected in the mutant depends on hedgehog (Hh) signalling, including the face and neural tube (Lewis et al., 1999; Buxton et al., 2004; Davey et al., 2006). Some aspects of the phenotype represent gain of Hh function (e.g. polydactyly), whereas others represent loss of Hh function (e.g. dorsalisation of the neural tube) (Davey et al., 2006). This complex phenotype can be understood in terms of the loss of both Gli repressor activity (limb polydactyly) and Gli activator activity (neural tube dorsalisation). *Gli3*$^{-/-}$ mouse mutants are polydactylous, whereas *Gli2*$^{-/-}$ mouse mutants have a dorsalised neural tube (Vortkamp et al., 1992; Matise et al., 1998).

The gene affected in the *talpid*^{3} chicken mutant is *KIAA0586*, which has a missense mutation predicted to truncate the protein at amino acid 366 (Fig. 1) (Davey et al., 2006). *KIAA0586* encodes a centrosomal protein necessary for the formation of primary cilia

[1]Biology and Biochemistry Department, University of Bath, Claverton Down, Bath BA2 7AY, UK. [2]Division of Developmental Biology, The Roslin Institute, The University of Edinburgh, Easter Bush, Midlothian, EH25 9RG, Scotland, UK. [3]Developmental Neurobiology, National Institute for Medical Research, Mill Hill, London NW7 1AA, UK.

*Author for correspondence (cat24@bath.ac.uk)

Accepted 16 May 2011

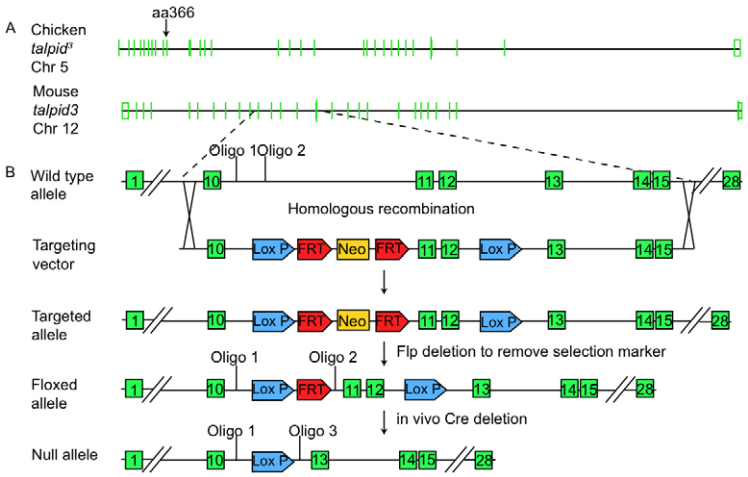

Fig. 1. Structure of chicken and mouse genes and strategy for generating a *talpid3*$^{-/-}$ mouse. (**A**) A comparison of the chicken *talpid*^{3} gene (*KIAA0586*, chromosome 5) with the mouse *talpid3* gene (*2700049A03Rik*, chromosome 12). Green bars represent exons. Arrow marks the exon that includes amino acid 366, which is mutated in chicken *talpid*^{3}, forming a premature stop codon. (**B**) Magnified region of mouse *talpid3* showing the cloning strategy for generating the *talpid3*$^{-/-}$ mouse. Shown are the loxP sites (blue) flanking exons 11 and 12 (green), FLP recognition target (FRT) sites (red) and the neomycin cassette (yellow) used as selection marker. Annealing sites of genotyping oligos are indicated.

(Yin et al., 2009). Since primary cilia are essential for Hh signalling and for the processing of Gli proteins in vertebrate cells, the absence of primary cilia on *talpid*^{3} mutant cells explains the defects seen in the chicken mutant.

The importance of primary cilia for Hh signalling emerged from a phenotypic screen, in which mouse mutants with Hh signalling defects were found to have mutations in genes encoding proteins required for intraflagellar transport (IFT), a process that builds and maintains the cilium (for a review, see Goetz and Anderson, 2010). This finding explains why patients with some rare ciliopathies have extra digits (Baker and Beales, 2009). Mice with mutations in genes encoding centrosomal proteins, including *Ftm* (*Rpgrip1l* – Mouse Genome Informatics), *Ofd1* and *Mks1*, also have polydactyly (Ferrante et al., 2006; Vierkotten et al., 2007; Weatherbee et al., 2009).

Here, we have generated a *talpid3*$^{-/-}$ mouse. Structure-function analysis of Talpid3 protein using rescue assays in *talpid*^{3} chicken mutant neural tubes has shown that the domain encoded by exons 11 and 12 is essential, although not sufficient, to rescue cilia and Hh signalling (Fig. 1) (Yin et al., 2009). We inserted loxP sites flanking this highly conserved region in the mouse *talpid3* gene to further test its functional significance and to allow us to conditionally remove *talpid3* function specifically in developing limbs in order to study later skeletogenesis, something that is difficult to study in chicken *talpid*^{3} mutants because of embryonic lethality.

MATERIALS AND METHODS

Embryos

Mutant mice were generated by Taconic Artemis (Cologne, Germany). E3.5 blastocysts from superovulated Balb/c females were injected with targeted C57BL/6 N.tac ES cells (Fig. 1) and transferred to pseudopregnant NMRI females. Highly chimeric mice were bred to C57BL/6 females and germline transmission identified by C57BL/6 (black) in offspring. The floxed allele was identified by PCR using oligo1 (5′-TGCCATGCAGGGATCATAGC-3′) and oligo2 (5′-GCTAGTACATTGCTGCAAGC-3′), which produce 351 bp and 470 bp products from the wild-type and floxed alleles, respectively (Fig. 1; see Fig. S1 in the supplementary material). Mice carrying the floxed allele were crossed with Gt(ROSA)26Sortm16 Cre mice to generate *talpid3*$^{-/+}$ mice; the null allele was identified by PCR using oligo1 and oligo3 (5′-GAGCACACTGGAGGAAAGC-3′), which produce a 273 bp product (Fig. 1; see Fig. S1 in the supplementary material); control oligos were fwd (5′-GAGACTCTGGCTACTCATCC-3′) and rev (5′-CCTTCAGCAAGAGCTGGGGAC-3′). Limb-specific *talpid3* knockout mice were generated by crossing female mice homozygous for the floxed allele with Prrx1-Cre males. *Prrx1-Cre; talpid3 lox* male offspring were backcrossed to female mice homozygous for the floxed *talpid3* allele; the *Cre* allele was identified by PCR using oligos fwd (5′-ACGACCAAGTGACAGCAATG-3′) and rev (5′-CTCGACCAGTTTAGTTACCC-3′).

talpid^{3} chicken carriers were maintained and genotyped as described (Davey et al., 2006).

Electron microscopy

Samples were fixed in 1.25% glutaraldehyde and 1% paraformaldehyde (PFA) in 80 mM sodium cacodylate buffer (pH 7.2) supplemented with 0.02% $CaCl_2$ for 2-3 hours at room temperature. Scanning electron microscopy (SEM) samples were washed in 100% acetone for 10 minutes, critical point dried, flushed five times, placed on carbon mounts, coated with Au/Pd and imaged using a Joel SEM6480LV scanning electron microscope. Samples for transmission electron microscopy (TEM) were prepared by the CHIPs facility at the Wellcome Trust Biocentre, Dundee, UK. Sections (70-100 nm) were viewed with a FEI Tecnai 12 transmission electron microscope.

Whole-mount RNA in situ hybridisation

Whole-mount in situ hybridisation was performed as described (Wilkinson and Nieto, 1993).

Section immunohistochemistry

Mouse embryos were fixed in 4% PFA for 2 hours at room temperature, embedded in 15% sucrose/7.5% gelatine and sectioned at 10 μm. Primary antibodies: rabbit anti-γ-tubulin, 1:100 (Sigma); mouse anti-acetylated tubulin, 1:100 (Sigma); mouse anti-Islet1, 1:10 [Developmental Studies Hybridoma Bank (DSHB)]; mouse anti-Nkx2.2, 1:5 (DSHB); mouse anti-Nkx6.1, 1:10 (DSHB); mouse anti-Pax6, 1:2 (DSHB); and mouse anti-Pax7, 1:10 (DSHB). Secondary antibodies used were anti-mouse IgG conjugated to Alexa-Fluor-488 and anti-rabbit IgG conjugated to Alexa-Fluor-546 at 1:500 (Molecular Probes). Samples were mounted with ProLong Gold plus DAPI (Invitrogen) and viewed with a Leica DMR compound microscope or a Zeiss LSM510 laser scanning confocal microscope.

Cell culture

Limbs from E12.5 mouse embryos were dissected in PBS, rinsed three times, transferred to 500 μl 1× trypsin (Sigma), finely minced using a razor blade and then agitated at 37°C to form a single-cell suspension. An equal volume of medium [DMEM:F12 (Gibco) containing 10% foetal calf serum, 1% L-glutamine and 1% Pen/Strep] was then added. Cells were washed and resuspended in 5 ml medium.

Immunohistochemistry of cultured cells

Cells were fixed in 4% PFA for 10 minutes, blocked in PBS containing 0.2% Tween 20 and 10% goat serum for 30 minutes, incubated with Alexa Fluor 488-phalloidin (1:40; Molecular Probes) or anti-vinculin primary antibody

(1:100; Sigma) for 1 hour at room temperature, then washed in PBS containing 0.2% Tween 20. Incubation with secondary antibody anti-mouse IgG conjugated to Alexa-Fluor-488 (1:500; Molecular Probes) was for 1 hour at room temperature. Samples were mounted with ProLong Gold plus DAPI and viewed with a Zeiss LSM510 confocal microscope.

Scratch assay and filming

Cells were seeded onto glass-bottom WillCo dishes (Intra Cell). When confluent, a scratch was made using a pipette tip. Filming was with a Zeiss LSM510Meta confocal microscope with an environment chamber.

Skeletal preparations

Mouse (Hogan and Lacy, 1994) and chicken (Tiecke et al., 2007) skeletal preparations were as described.

Histology

Samples were fixed in 4% PFA overnight, dehydrated into Histo-Clear (National Diagnostics) and wax embedded. Sections (5 μm) were stained with Hematoxylin and Eosin and photographed using a Leica DMR compound microscope.

Section in situ hybridisation

Section in situ hybridisation was performed as described (Moorman et al., 2001).

Optical projection tomography (OPT) scanning

Embryos and limb skeletons processed as described (Fisher et al., 2008) were scanned with a Bioptonics 3001 OPT scanner. Isosurfaces were generated for limbs and skeletons, limbs cropped, overlaid, and width, length and volume measurements and movies made using Amira 5.2.2 software. Mean hand plate volume was calculated by cropping the limb at its narrowest point, determining the number of voxels with signal over a set threshold and multiplying by voxel size.

RESULTS

talpid3$^{-/-}$ mice show embryonic lethality, abnormal Shh signalling and lack primary cilia

To test whether exons 11 and 12 are essential for *talpid3* function in the mouse they were flanked by loxP sequences (Fig. 1B). C57BL/6 mice carrying the floxed allele were crossed with mice from a line ubiquitously expressing Cre recombinase (see Materials and methods). Embryos homozygous for the *talpid3* deletion (*talpid3*$^{-/-}$) survived until embryonic day (E) 10.5, but did not develop significantly beyond E9.5 – turning was not completed (Fig. 2B, compare with wild-type littermate in 2A) – and exhibited pericardial oedema and significant haemorrhaging (Fig. 2B, arrow and arrowhead; see Fig. S2 in the supplementary material), similar to the vascular defects observed in *talpid*^{3} chicken (Davey et al., 2007). Heterozygous C57BL/6 *talpid3*$^{-/+}$ mice were crossed with CD1 mice. *talpid3*$^{-/-}$ embryos with this mixed background developed until E10.5, underwent turning and formed limb buds (Fig. 2C). These mice exhibited external defects reflecting abnormal Shh signalling, with narrower heads and fused medial and lateral nasal processes creating a frontal process and nasal pit across the midline (Fig. 2D′,D″, compare with wild type in 2D), as demarcated by *Fgf8* expression (Fig. 2E′,F′, compare with wild type in 2E,F). Defects were also found in other regions dependent on Shh signalling: the neural tube was dorsalised, as shown by loss of Nkx2.2 and Islet1 and reduced Nkx6.1 expression (Fig. 2G′-I′, compare with wild type in 2G-I), accompanied by ventral expansion of Pax6 and Pax7 expression (Fig. 2J,K′, compare with wild type in 2J,K). Furthermore, cilia can be seen projecting from centrosomes of wild-type neural tube cells (Fig. 2L, arrows) whereas no cilia could be detected projecting from centrosomes in cells in *talpid3*$^{-/-}$ neural tube (Fig. 2L′, arrowheads). TEM of sections through *talpid3*$^{-/-}$ mouse neural tube showed that

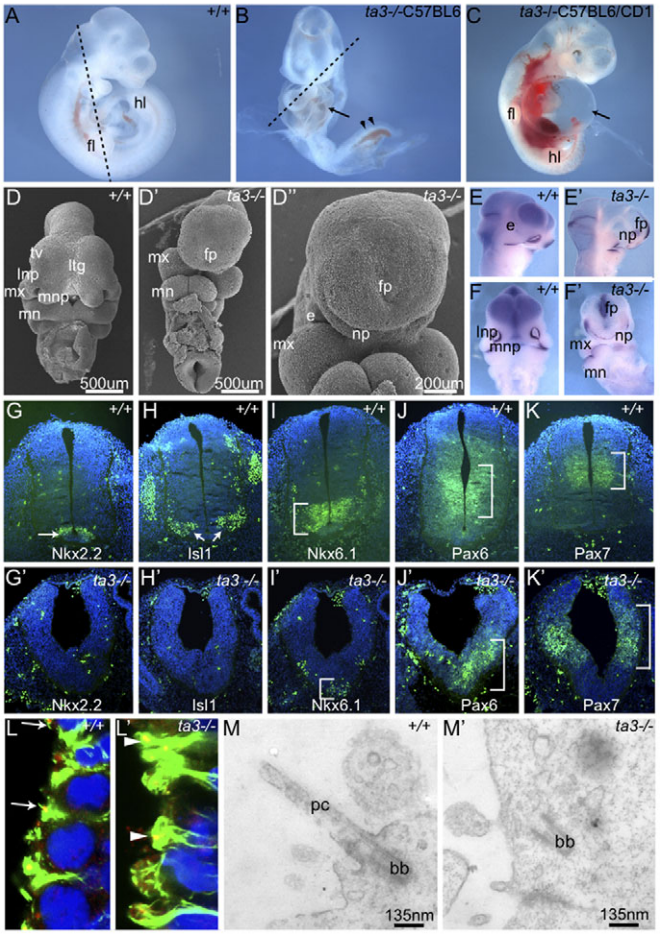

Fig. 2. Phenotype of *talpid3*$^{-/-}$ mouse embryos. (**A-C**) Mouse E10.5 wild-type (A) and *talpid3*$^{-/-}$ (B) littermates on C57BL/6 background, or *talpid3*$^{-/-}$ on C57BL/6/CD1 mixed background (C). Arrow indicates pericardial oedema; arrowheads indicate haemorrhaging. fl, forelimb; hl, hind limb. The dashed line indicates the plane of sections shown in Fig. S2 in the supplementary material. (**D-F′**) Scanning electron micrographs (D-D″) and whole-mount *Fgf8* in situ hybridisation (E-F′) at E10.5 showing loss of midline facial structures in *talpid3*$^{-/-}$ embryos. e, eye; fp, frontal process; ltg, lamina terminalis groove; lnp, lateral nasal process; mn, mandibular process; mx, maxillary process; mnp, medial nasal process; np, nasal pit; tv, telencephalic vesicle. (**G-K′**) Transverse sections through E10.5 neural tube stained with antibodies to neural transcription factors (green); nuclei are counterstained with DAPI (blue). Expression of the ventral markers Nkx2.2 and Islet1 (arrows) is lost and Nkx6.1 (bracket) is reduced in *talpid3*$^{-/-}$ embryos (compare G-I with G′-I′). Expression of the dorsal markers Pax6 and Pax7 (brackets) is expanded in *talpid3*$^{-/-}$ embryos (compare J,K with J′,K′). (**L,L′**) Transverse section through the neural tube. In wild type (L), cilia axonemes (arrows; stained for acetylated tubulin, green) project into the lumen from centrosomes (stained for γ-tubulin, red), whereas no axonemes project from centrosomes (arrowheads) in *talpid3*$^{-/-}$ mutant cells (L′). (**M,M′**) Transmission electron micrographs of transverse sections though neural tube show primary cilium (pc) projecting into the lumen of a wild-type cell (M). The basal body (bb) is at the apical surface of a *talpid3*$^{-/-}$ cell but is not docked (M′).

centrosomes fail to dock with the apical cell membrane in *talpid3*$^{-/-}$ mouse cells (Fig. 2M′, compare with wild-type cilium in 2M). Thus, deleting *talpid3* exons 11 and 12 in the mouse leads to the loss of primary cilia and to face and neural tube defects similar to those seen in *talpid*^{3} chicken mutants (Table 1).

Table 1. Comparison of *talpid*^{3} chicken and *talpid3*$^{-/-}$ mouse embryos

Phenotype	*talpid*^{3} chicken	*talpid3*$^{-/-}$ mouse
Loss of cilia	Yes, centrosome fails to dock with plasma membrane	Yes, centrosome fails to dock with plasma membrane
Lethality	HH28, 6 days of development (equivalent to E12.5 in mouse)	Develop to E9.5 (equivalent to HH19 in chicken)
Neural tube patterning	Dorsalised	Dorsalised
Facial development	Loss of midline structures	Loss of midline structures
Left right asymmetry	Normal	Randomised

Comparison of the limb at day 10/11 in chicken and E17.5 in mouse

	talpid^{3} chicken		*talpid3* CKO mouse	
Phenotype	Wing	Leg	Forelimb	Hind limb
Polydactyly	Yes	Yes	Yes (up to 9 digits)	Yes (6 digits)
Syndactyly	Cartilaginous syndactyly	Cartilaginous and soft tissue syndactyly	Soft tissue syndactyly only	Soft tissue syndactyly only
Endochondral ossification	No	No	No	No
Proximodistal growth and patterning	Elements are short	Elements are short	Elements are short, loss of phalanx	Elements are short, loss of phalanx
Anteroposterior patterning	None	None	None	None
Digit identity	None	None	None	Digit 4 present?
Zeugopod	Radius and ulna fused	Fibula and tibia fused	Radius and ulna separate	Fibula and tibia separate
Autopod	Carpals and metacarpals fused	Tarsals fused, metatarsals fused or separate	Carpals and metacarpals fused or separate	Tarsals and metatarsals fused or separate

talpid^{3} chicken mutant embryos showed normal left/right axis specification (normal heart looping, *n*=87, stage 20HH-24HH; normal liver lobe specification and stomach turning, *n*=2, day 10), whereas heart looping was abnormal in *talpid3*$^{-/-}$ mouse embryos (Table 1). In all E10.5 wild-type mouse embryos examined (*n*=10), the heart looped into a curved tube with the convex surface directed toward the right, whereas heart looping in *talpid3*$^{-/-}$ mouse embryos was sometimes to the right (2/10), sometimes to the left (5/10), and in some cases to neither left nor right (3/10) (Fig. 3, compare A with A′). In E8.0 [1- to 7-somite (s)] wild-type mouse embryos, Nodal is expressed around the node but more highly on the left side and in the left lateral plate mesoderm (Brennan et al., 2001), but in the *talpid3*$^{-/-}$ mouse embryo (4s), expression was detected in the node and in both the left and right lateral plate mesoderm with stronger expression on the right (Fig. 3, compare B with B′); two other mutant embryos at 4-5s showed equal levels of Nodal expression on both sides of the node. A more detailed analysis of the expression of genes involved in left/right asymmetry will be published elsewhere. Lack of left/right asymmetry in *talpid3*$^{-/-}$ mouse embryos can be explained by the lack of nodal cilia (Fig. 3, compare C-E with C′-E′; *n*=4).

Patterning and skeletogenesis of *talpid3* conditional knockout (CKO) mouse limbs

To study the loss of *talpid3* function specifically in limbs, we crossed mice with floxed *talpid3* exons 11 and 12 with mice from the Prrx1-Cre strain. Prrx1-Cre is expressed in forelimb mesenchyme from E9.5 and in hind limb mesenchyme from E10.5 (Logan et al., 2002). Sections through E9.5 *talpid3* CKO fore- and hind limbs showed cilia on both mesenchyme and ectoderm cells (Fig. 4C; data not shown), but by E10.5 cilia were absent from all mesenchyme cells in forelimbs (Fig. 4D, arrowheads, compare with wild type in 4A) whereas 2% of hind limb mesenchyme cells still had a cilium (Fig. 4E). By contrast, cilia were detected on ectoderm cells of both fore- and hind limbs at E10.5 (Fig. 4D,E, arrows), indicating that *talpid3* function is abolished specifically in mesenchyme cells. Loss of cilia was also readily observed in

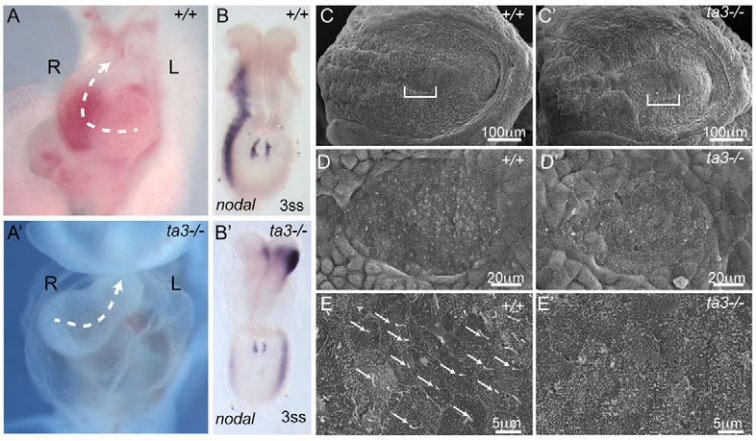

Fig. 3. Left/right asymmetry in wild-type and *talpid3*$^{-/-}$ mouse embryos. (**A**,**A′**) Wild-type mouse embryo heart loops to the right (A), whereas heart looping is randomised in *talpid3*$^{-/-}$ mouse embryos; an example of looping to the left is shown (A′). Dashed arrows indicate the direction of looping; R, right; L, left. (**B**,**B′**) *Nodal* is expressed in left lateral plate mesoderm of wild-type embryos (B), and in both the left and right lateral plate mesoderm of *talpid3*$^{-/-}$ embryos (B′). ss, somite stage. (**C-E′**) Scanning electron micrographs (increasing magnification top to bottom) of E8.0 node (brackets). (C-E) A primary cilium is present on almost every cell in the wild-type node (arrows). (C′-E′) Cilia are absent from the *talpid3*$^{-/-}$ node.

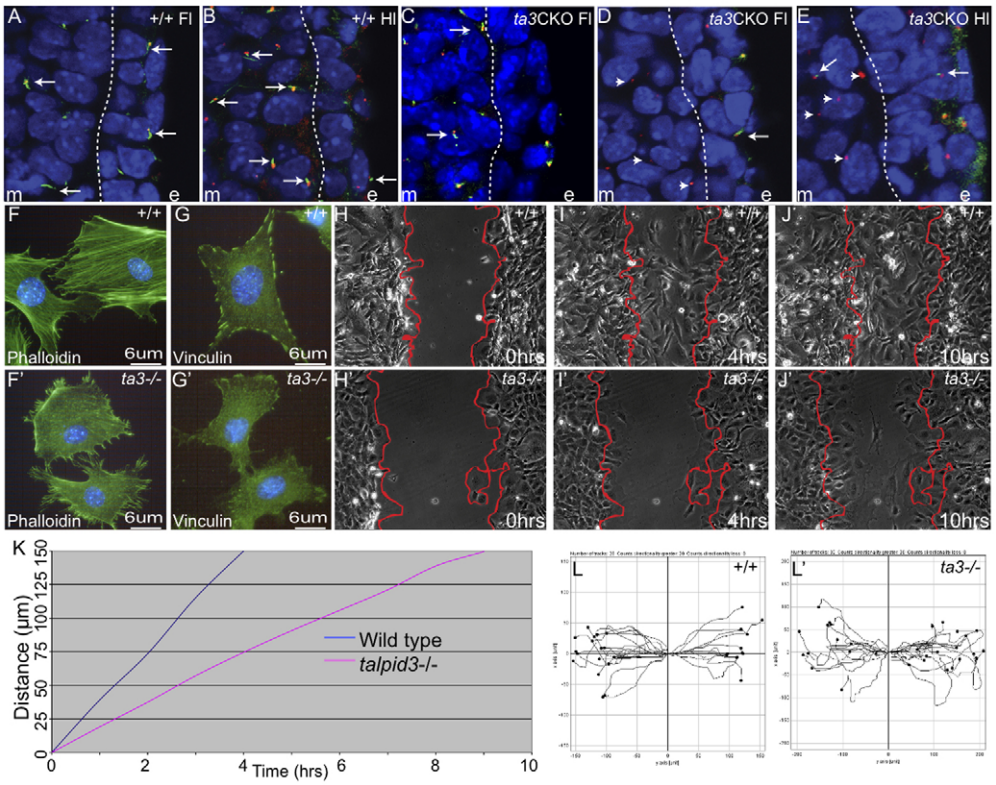

Fig. 4. Loss of cilia from cells of *talpid3* CKO mouse limbs. (**A**,**B**) Wild-type mouse forelimb (A) and hind limb (B). Primary cilia axonemes (arrowed; stained for acetylated tubulin, green) project from centrosomes (stained for γ-tubulin, red) on mesenchyme and ectoderm cells. (**C**) *talpid3* CKO forelimb at E9.5, showing cilia (arrows). (**D**) *talpid3* CKO forelimb at E10.5. Primary cilia are absent from mesenchyme cells (arrowhead shows centrosome), but present on ectoderm cells (arrows). (**E**) *talpid3* CKO hind limb at E10.5; 2% of mesenchyme cells have primary cilium (arrow). Fl, forelimb; Hl, hind limb; m, mesenchyme and e, ectoderm, separated by dashed line. (**F**,**F′**) Phalloidin marks stress fibres (green) in wild-type mouse limb fibroblasts (F), which are reduced in *talpid3*$^{-/-}$ fibroblasts (F′); also note the increased number of filopodia around the cell circumference. (**G**,**G′**) Vinculin staining marks focal adhesions in wild-type mouse limb fibroblasts (G), which are absent in *talpid3*$^{-/-}$ fibroblasts (G′). (**H-J′**) Still images from film of scratch assay. Wild-type mouse limb fibroblasts migrate to close the scratch (delimited by red lines) within 10 hours (H-J), whereas *talpid3*$^{-/-}$ fibroblasts migrate more slowly (H′-J′). (**K**) The migration speed of wild-type mouse limb fibroblasts as compared with *talpid3*$^{-/-}$ fibroblasts. (**L**,**L′**) Plots tracing the movement of wild-type mouse limb fibroblasts (L) or *talpid3*$^{-/-}$ fibroblasts (L′) away from the scratch edge show that *talpid3*$^{-/-}$ fibroblasts lack directionality.

cultured fibroblast cells generated from E12.5 fore- and hind limbs, with only 6% of mutant fibroblasts having cilia after 48 hours of serum starvation, as compared with 74% of wild-type fibroblasts (see Fig. S3A,A′ in the supplementary material). *talpid3* CKO mouse fibroblasts, like *tapid*[3] chicken mutant fibroblasts, had fewer stress fibres and focal adhesions than wild-type fibroblasts (Fig. 4, compare F,G with F′,G′) and also took longer to close a scratch (Fig. 4, compare H-J with H′-J′), migrating more slowly (Fig. 4K) and with less directionality (Fig. 4, compare L with L′).

talpid3 CKO mouse forelimbs were polydactylous, with up to nine digits (Fig. 5A′; compare Movies 1 and 2 in the supplementary material; see Fig. S4A in the supplementary material), which appeared, externally, to be fused (Fig. 5, compare insets in A′ and A). Skeletal preparations revealed, however, only soft tissue syndactyly. Up to 16 carpals developed, compared with seven in wild-type mouse wrist, and were sometimes fused (see Fig. S4B,B′ in the supplementary material; Table 2). Nearly all the digits appeared morphologically similar, usually consisting of two rather than three phalanges, including a terminal phalanx, and some digits were bifurcated (Fig. 5A′, arrow; Table 2). *talpid3* CKO mouse hind limbs were less affected than forelimbs, with usually just one extra digit, and digits also bifurcated (Fig. 5B′; compare Movies 3 and 4 in the supplementary material; see Fig. S4C in the supplementary material; Table 2). As in mutant forelimbs, most hind limb digits only had two phalanges, although in several cases the penultimate posterior digit developed three phalanges (Fig. 5B′, asterisk; Table 2) and the most posterior metatarsal was of wild-type shape (Fig. 5B′, arrowhead).

In addition to being polydactylous, *talpid3* CKO mouse limbs were short, with each skeletal element in both fore- and hind limbs being 40-70% shorter than wild-type counterparts (Fig. 6A), and the ossification of fore- and hind limb elements was abnormal and absent in digits at E17.5 (Fig. 5, compare Alizarin Red staining in A′,B′ with that in A,B). Histological analysis of sections through growth plates confirmed that there was no subperiosteal bone deposited in the radius and ulna in mutant forelimbs; consequently, no bone collar formed, although calcified tissue stained with Alizarin Red formed internally (Fig. 6, compare wild type in B with *talpid3* CKO in B′). Growth plates in long bones of *talpid3* CKO forelimbs showed an increase in resting chondrocytes and a reduction in columnar chondrocytes and prehypertrophic chondrocytes, although chondrocytes in the long-bone centre still eventually underwent hypertrophy (Fig. 6, compare C with C′, proximal growth plate of ulna). Sections through digits at E17.5

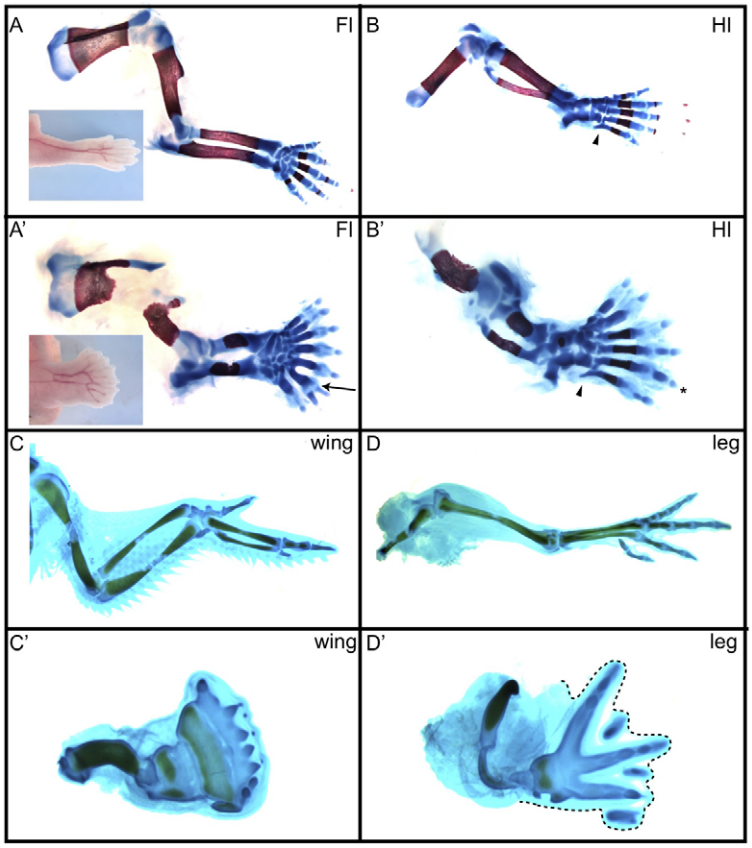

Fig. 5. Skeletal patterns in wild-type and *talpid3* CKO mouse limbs. (**A-B'**) E17.5 wild-type (A,B) and *talpid3* CKO (A′,B′) mouse forelimb (Fl) and hind limb (Hl) stained with Alcian Blue for cartilage and Alizarin Red for calcified tissue. The *talpid3* CKO mouse forelimb and hind limb show polydactyly. Arrow (A′) indicates bifurcated digit. Asterisk (B′) indicates penultimate posterior digit with normal morphology. Arrowheads indicate normal posterior metatarsal (compare B with B′). Insets show wild-type (in A) and *talpid3* CKO (in A′) forelimbs at E17.5; note the soft tissue syndactyly in the *talpid3* CKO forelimb. (**C-D'**) Day 11 wild-type (C,D) and *talpid*^{3} (C′,D′) chicken wing and leg stained with Alcian Blue. Note the cartilaginous syndactyly in the *talpid*^{3} chicken wing and leg (dotted line marks edge of limb).

confirmed the ossification failure (Fig. 6, compare wild type in D with *talpid3* CKO in D′, asterisk) and showed expansion of the joint-forming region (Fig. 6D′, bracket). Morphological changes in joints are presaged by alterations in *Gdf5* expression (Storm and Kingsley, 1999), which, in E13.5 wild-type forelimbs, precisely marked the joints (Fig. 6E), but in *talpid3* CKO forelimbs was more diffuse, encompassing a larger area (Fig. 6E′).

The general features of *talpid3* mouse CKO limbs resembled those of the *talpid*^{3} chicken mutant. *talpid*^{3} chicken mutant embryos surviving until day 10 have short wings and legs with an increased number of morphologically similar digits, although phalange number varies and ossification is impaired (Fig. 5C′,D′) (see also Ede and Kelly, 1964b; Macrae et al., 2010). In *talpid3* CKO mouse forelimbs, digit cartilages were separate, with only soft tissue syndactyly, whereas in *talpid*^{3} chicken mutant wings digit cartilages are fused (Fig. 5, compare C′ with A′). In *talpid*^{3} chicken mutant legs, the extent of syndactyly is variable, with fusion of digit cartilages in some cases but only soft tissue syndactyly in others (Fig. 5D′) (see also Ede and Kelly, 1964b).

Patterning defects and skeletal defects in *talpid3* CKO mouse limb buds, as in *talpid*^{3} chicken mutant limb buds, can be ascribed to an inability to respond to Shh and Indian hedgehog (Ihh) signalling, respectively, as reflected in changes in the expression of Gli-regulated genes. At E10.5, *Shh* was expressed in the polarising region of *talpid3* CKO mouse forelimb buds as in wild type (Fig. 7A,A′), but expression of the Gli activator targets *Ptch1* and *Gli1* was lost (Fig. 7, compare B,C with B′,C′), whereas expression of Gli repressor targets, such as *Hoxd13*, was expanded anteriorly (Fig. 7D,D′, arrowheads) as was gremlin (*Grem1* – Mouse Genome Informatics) (Fig. 7E,E′, arrowheads). *Bmp4*, which is normally expressed in the anterior limb bud, was reduced (Fig. 7F,F′). By contrast, the expression of genes upstream of Shh signalling, for example *Hand2*, was unaffected (Fig. 7G,G′), as was the expression of genes involved in proximodistal patterning, such as *Hoxa11* and *Fgf8* (Fig. 7, compare H,I with H′,I′), although *Hoxa13* expression was expanded anteriorly (Fig. 7J,J′). Sections of *talpid3* CKO humerus at E13.5 showed that *Ihh* is expressed in prehypertrophic chondrocytes as in wild type, but the absence of hypertrophic chondrocytes in the middle of the rudiment at this stage led to a single central zone of *Ihh*-expressing cells, whereas in wild type two zones were separated by hypertrophic chondrocytes no longer expressing *Ihh* (Fig. 6F,F′). At E13.5, *Ptch1* was expressed in the perichondrium surrounding developing digits in wild-type forelimbs, but no expression was detected in *talpid3* CKO (Fig. 6G,G′).

Morphogenesis and digit spacing in *talpid3* CKO mouse limbs

To compare limb shape, optical projection tomography (OPT) was used to generate 3D images of wild-type and *talpid3* CKO forelimbs from E11.5-13.5 (Fig. 8A-C). By E11.5, hand plates of *talpid3* CKO forelimbs were already slightly broader than those of the wild type (Fig. 8Ab,D; see D′, which shows where width measurements of the hand plate were taken), and by E12.5 hand plates of *talpid3* CKO forelimbs were clearly broader both anteriorly and posteriorly (Fig. 8Bb,D). *talpid3* CKO hand plates became broader still by E13.5, but distal outgrowth was reduced compared with wild type (Fig. 8Cb,D). Digital slices show that *talpid3* CKO hand plates were of comparable thickness to those of the wild type until E13.5, when the mutant expanded more ventrally than the wild type (Fig. 8Ac-Ce, arrows). The mean volume (±s.d.) of the hand plate at E11.5 was 395±76 mm^{3} (n=14) for wild type

Table 2. Analysis of limb development in E17.5 *talpid3* CKO mouse and day 10/11 *talpid*^{3} chicken embryos

Genotype*	Number of carpals†/tarsals‡	Number of metacarpals†/metatarsals‡	Number of metacarpals†/metatarsals‡ with secondary ossification	Number of digit tips	Number of phalanges§
Mouse					
Right forelimb					
Wild type	7	5	4	5	23333
a	16	7	0	8	22222222
b	9	7	0	7	2222222
c	8	8	0	8	22222222
d	12	8	0	9	222222222
e	9	7	0	8	22222233
Left forelimb					
Wild type	7	5	4	5	23333
b	7	7	0	9	222222222
c	6	7	0	8	22222222
d	7	8	0	8	22222222
e	7	6	0	8	12222222
Right hind limb					
Wild type	8	5	4	5	23333
a	7	6	4	6	222323
b	4	5	3	5	22332
c	7	5	4	6	122232
d	10	6	3	6	222332
e	7	6	3	6	112232
Left hind limb					
Wild type	8	5	4	5	23333
b	6	5	3	6	222232
c	6	6	3	6	222332
d	5	5	4	6	232222
e	7	6	3	6	111222
Chicken					
Wing					
Wild type	2	3	2	3	221
a	Fused	Fused	0	9	101110100
b	Fused	Fused	0	ND	ND
c	Fused	Fused	0	ND	ND
Leg					
Wild type	2	3	3	4	2234
a	Fused	3	0	6	212111
b	Fused	6	0	7	0022123
c	Fused	4	0	5	21121

*a-e refer to different individual limb specimens of mouse *talpid3*$^{-/-}$ or chicken *talpid*^{3}.
†Mouse forelimb or chicken wing.
‡Mouse hind limb or chicken leg.
§The number of phalanges including the terminal phalanx is given (0-4), in turn, for each digit tip.
ND, not determined.

and 547±179 mm^3 (n=12) for *talpid3* CKO (P=0.0158, t-test). At E12.5, the mean volumes of the wild-type and *talpid3* CKO hand plates were 804±215 mm^3 (n=6) and 1074±401 mm^3 (n=6), respectively (P=0.2182, t-test). Assuming each digit occupies the same space, this would give 160.8 mm^3 per digit in E12.5 wild-type forelimbs with five digits, but only 134.25 mm^3 per digit in *talpid3* CKO forelimbs with an average of eight digits.

A striking feature of the *talpid3* digit phenotype is syndactyly, involving only soft tissue in mouse but cartilaginous fusion in chicken *talpid*^{3} wing and sometimes leg. We investigated the formation of digital condensations and interdigital spaces in *talpid3* CKO mutant mouse limbs. Wild-type and *talpid3* CKO littermates were collected between E11.5 and E13.5 (E11.5 n=4 litters; E12.5 n=3 litters; E13.5 n=3 litters) and *Sox9* expression in the left forelimbs of each embryo and *Raldh2* (*Aldh1a2* – Mouse Genome Informatics) expression in right forelimbs was analysed. *Sox9* is expressed in prechondrogenic cells and is required for cartilage differentiation (Akiyama et al., 2002), whereas *Raldh2* is expressed in interdigital spaces between digit cartilage condensations (Niederreither et al., 1997; Schmidt et al., 2009; Kuss et al., 2009). Based on the patterns of expression obtained, the sequence of formation of digit condensations and interdigital spaces in wild-type and *talpid3* CKO limbs was deduced.

In wild-type E11.5 mouse forelimbs, *Sox9* was expressed throughout the digital plate. Then, first a *Sox9*-positive digit 4 condensation became discernible (Fig. 8E, asterisk), followed by rapid breakup of continuous *Sox9* expression into digit 2 and 3 condensations, then digit 5, then digit 1 condensations (Fig. 8G);

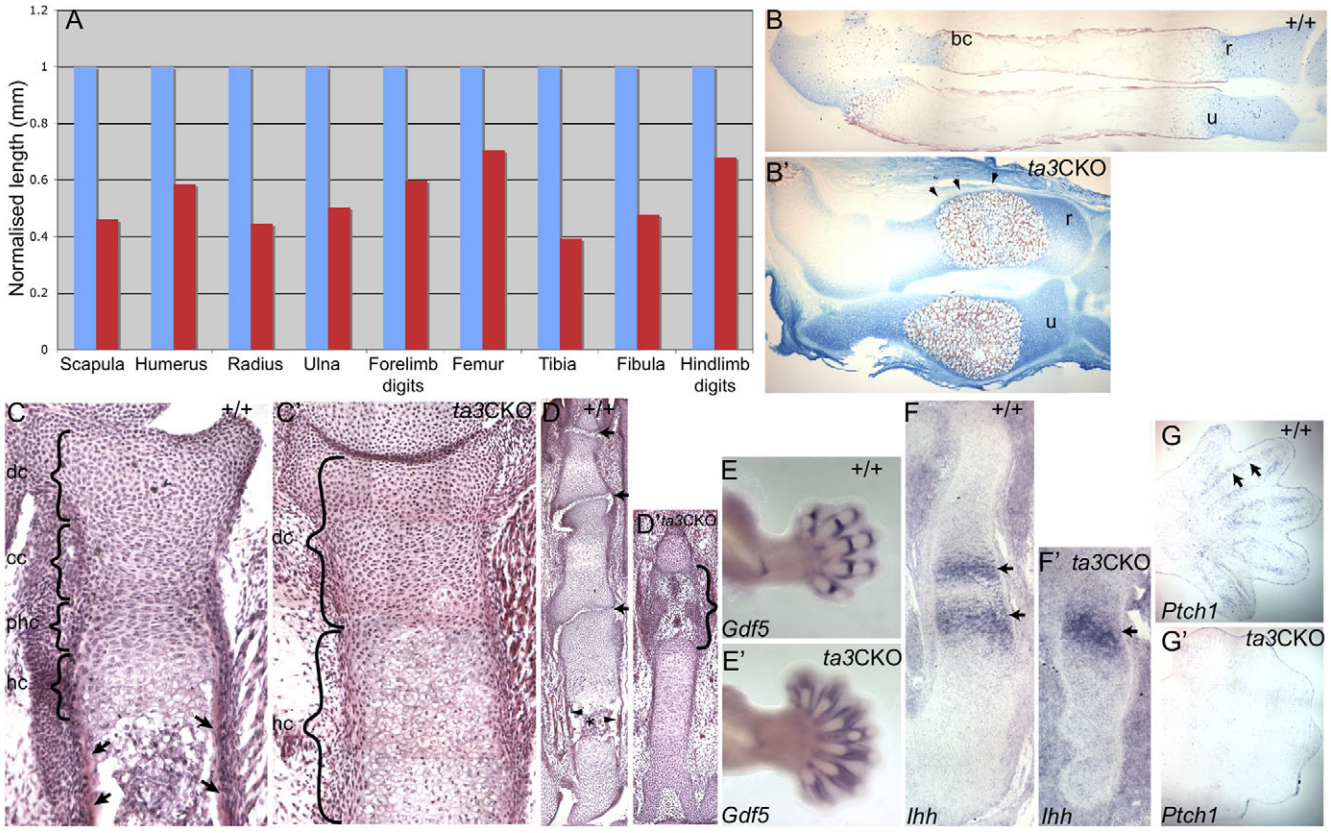

Fig. 6. Skeletogenesis in wild-type and *talpid3* CKO mouse limbs. (**A**) The length of *talpid3* CKO skeletal elements (red) as a percentage of wild-type elements (blue) normalised to one. (**B**,**B′**) Wild-type (B) and *talpid3* CKO (B′) mouse radius (r) and ulna (u), with cartilage stained with Alcian Blue at ends of elements, and bony collar (bc) stained with Alizarin Red. In *talpid3* CKO radius and ulna, cartilage is present at the ends of elements and also surrounds the Alizarin Red-stained (arrowheads) central region of calcified tissue. (**C**,**C′**) Longitudinal section through the proximal growth plate of wild-type (C) and *talpid3* CKO (C′) ulna stained with Hematoxylin and Eosin. Brackets indicate different zones: dc, dividing chondrocytes; cc, columnar chondrocytes; phc, prehypertrophic chondrocytes; hc, hypertrophic chondrocytes; arrows indicate subperiosteal bone. Note only dividing and hypertrophic chondrocytes and no subperiosteal bone in *talpid3* CKO ulna. (**D**,**D′**) Sections of middle digit stained with Hematoxylin and Eosin. Note defined joints (arrows), ossification (asterisk) and subperiosteal bone (arrowhead) in wild type (D), whereas the *talpid3* CKO digit has an enlarged joint-forming region (bracket, D′). (**E**,**E′**) *Gdf5* expression marks joints in wild-type (E) and *talpid3* CKO (E′) forelimbs at E13.5. (**F**,**F′**) Longitudinal section through humerus showing *Ihh* expression (dark blue) in two bands (arrows) of prehypertrophic chondrocytes in wild type (F) but in only a single band (arrow) of hypertrophic like-chondrocytes in *talpid3* CKO humerus (F′). (**G**,**G′**) *Ptch1* is expressed (arrows) in perichondrium surrounding digits in wild-type hand plate (G) but is absent in *talpid3* CKO hand plate (G′).

Zhu et al. (Zhu et al., 2008) reported digit condensation in the order 4, 2, 5, 3, 1 using a *Nog-lacZ* knock-in allele to detect condensations rather than *Sox9* expression. At the same time, *Raldh2* was expressed in the mid region of the bud tip (Fig. 8F), then separated into two blocks of expression representing the second and third interdigital spaces (Fig. 8H). At E12.5, all five digit condensations had formed in the forelimb (Fig. 8I,K) and the second, third and fourth interdigital regions were present, with the first interdigit following later (Fig. 8J). *Raldh2* expression was then detected anterior to digit 1 and posterior to digit 5 (Fig. 8L). By E13.5, the *Sox9* expression pattern mirrored digit shape (Fig. 8M); *Raldh2* expression became restricted to digit/interdigit boundaries (Fig. 8N). The spacing between digits was even in all wild-type forelimbs analysed.

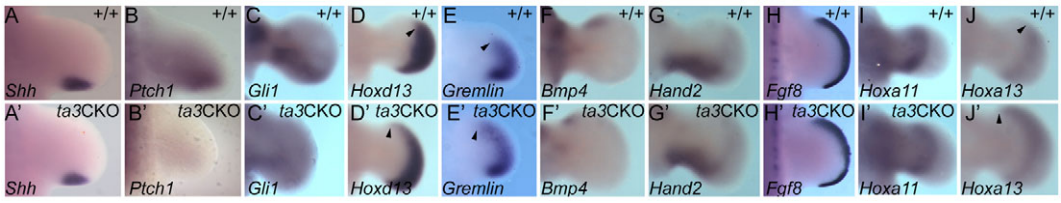

Fig. 7. Gene expression in wild-type and *talpid3* CKO mouse limbs. (**A-J′**) Whole-mount in situ hybridisation for the indicated genes in wild-type (A-J) and *talpid3* CKO (A′-J′) mouse forelimb at E10.5 (A-B′) and E11.5 (C-J′). Limbs viewed from dorsal side, anterior up. Arrowheads indicate anterior extension of gene expression in *talpid3*$^{-/-}$ limb buds compared with wild type.

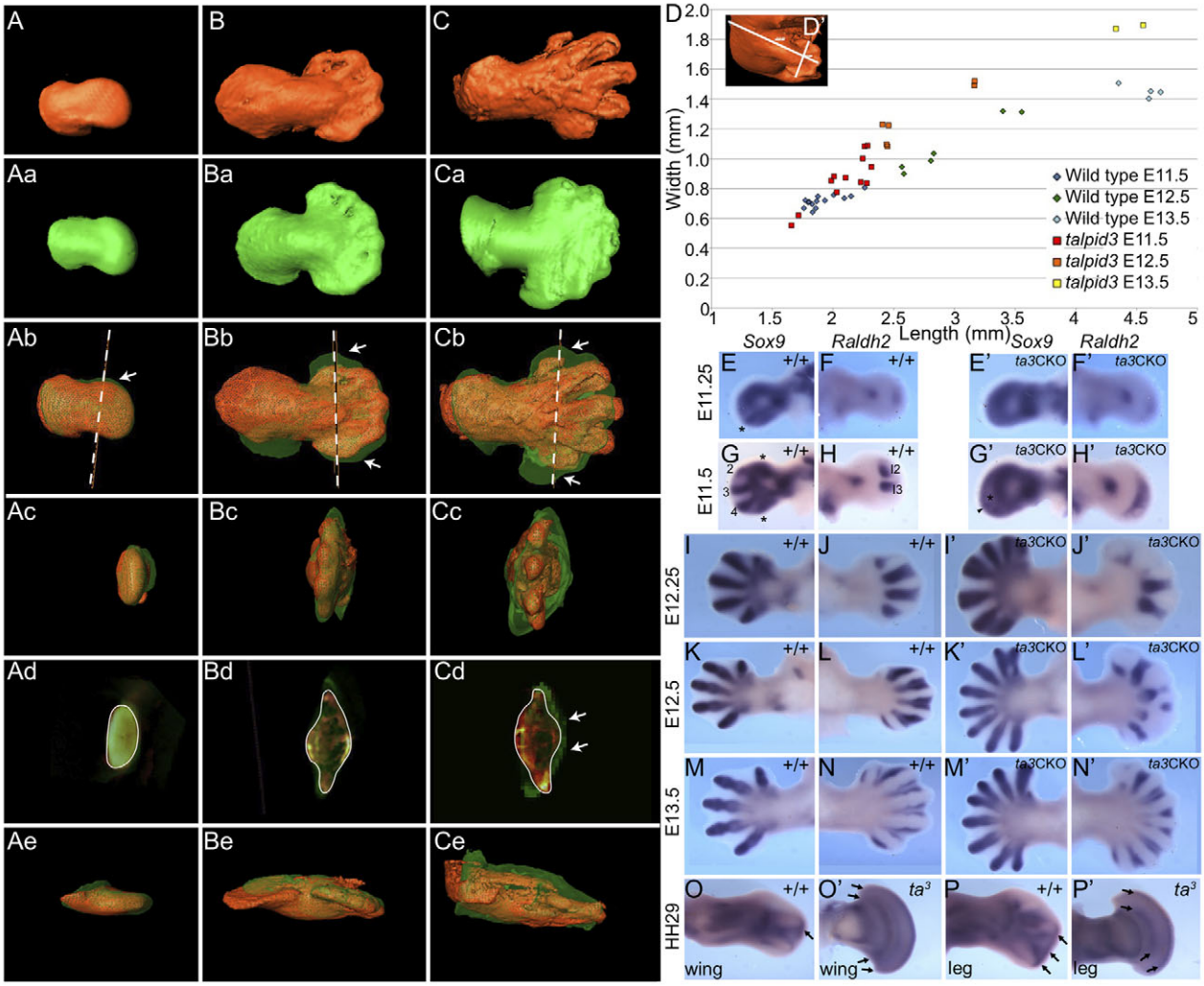

Fig. 8. Limb bud shape and digit spacing in wild-type and *talpid3* CKO mouse limbs. (**A-Ce**) Three-dimensional surfaces of right forelimbs from wild-type (A-C, red) and *talpid3* CKO (Aa-Ca, green) mice. A-Ae, E11.5; B-Be, E12.5; C-Ce, E13.5. Overlaid limbs (Ab-Cb) show the difference (arrows) in shape between wild type (red mesh) and *talpid3* CKO (transparent green) hand plates. Dashed line indicates the plane of sections in Ad-Cd. (Ac-Cc) Overlaid limbs viewed from a distal perspective. (Ad-Cd) Digital sections show that *talpid3* CKO limbs are thickened ventrally at E13.5 (arrows). (Ae-Ce) Overlaid limbs viewed from the anterior. (**D**,**D′**) Scatter plot (D) showing increasing hand plate width over limb length (measured from limb tip to spine, see D′) in *talpid3* CKO forelimbs. (**E**,**G**,**I**,**K**,**M**) *Sox9* expression in wild-type left forelimb from E11.5 to E13.5. Digit-forming condensations are marked with an asterisk (E,G) or numbered (G). (**E′**,**G′**,**I′**,**K′**,**M′**) *Sox9* expression in *talpid3* CKO left forelimb from E11.5 to E13.5. Region with reduced *Sox9* expression is marked with an asterisk (G′), and the first digit condensation is marked with an arrowhead (G′). (**F**,**H**,**J**,**L**,**N**) *Raldh2* expression in wild-type left forelimb from E11.5 to E13.5. Interdigits are numbered (H). (**F′**,**H′**,**J′**,**L′**,**N′**) *Raldh2* expression in *talpid3* CKO left forelimb from E11.5 to E13.5. (**O**,**P**) *Raldh2* expression in wild-type chicken wing (O) and leg (P). Expression is present in the interdigit and between the digit tip and apical ectodermal ridge (arrows). (**O′**,**P′**) *Raldh2* expression in *talpid*^{3} chicken wing (O′) and leg (P′). Note *Raldh2* expression in a thin line between metacarpals/metatarsals and phalanges as well as beneath the apical ectodermal ridge (arrows), but no interdigital *Raldh2* expression. Limbs viewed from dorsal side, anterior up.

In *talpid3* CKO mouse limbs, digit condensation was delayed by 6-12 hours, interdigital spaces were not so precisely defined and digit spacing was not always so regular. Thus, whereas in E11.5 wild-type littermates digit 2, 3 and 4 condensations were apparent and discrete and the second and third interdigital spaces had formed, in *talpid3* CKO limb buds *Sox9* expression remained throughout the digital plate, although with weaker expression in the mid-posterior region at the limb tip (Fig. 8E′,G′, asterisk). *Raldh2* expression was increased, spreading diffusely throughout the mid-posterior limb region where *Sox9* expression is reduced (Fig. 8F′,H′). Digit condensations expressing *Sox9* first appeared in the posterior of *talpid3* CKO forelimbs (Fig. 8G′, arrowhead), followed by rapid breakup of *Sox9* expression as seen in wild-type forelimbs, resulting in many *Sox9*-expressing condensations throughout the broad digital plate (Fig. 8I′-M′). These condensations were not always evenly spaced; *Raldh2* expression could be fragmented, not always extending from proximal to distal throughout the digital plate (Fig. 8J′-N′), consistent with the interdigital spaces not forming as regularly as in wild type.

We also examined *Raldh2* expression in *talpid*^{3} chicken mutant wings and legs, which can show more severe syndactyly. In wild-type HH29 chicken wings and legs, *Raldh2* was expressed in the interdigital spaces as in mouse, but also in a thin band just beneath

the apical ectodermal ridge (Fig. 8O,P, arrows). In *talpid*^{3} chicken mutant wings and legs at HH29, *Raldh2* was expressed in a continuous band around the rim and in another continuous band between the fused phalanges and fused metacarpals/metatarsals (Fig. 8O′,P′, arrows). Thus, *Raldh2* expression is continuous in *talpid*^{3} chicken mutant wings and legs at a stage when interdigital spaces expressing *Raldh2* have formed in wild type.

DISCUSSION

Deletion of the highly conserved exons 11 and 12 of *talpid3* in the mouse abolishes its function and leads to a lack of primary cilia and hence abnormal Hh signalling. This extends our previous finding that these two exons are essential, but not sufficient, to rescue *talpid*^{3} function in the chicken and is the first time that a null mouse has been generated based on work on a chicken mutant. Our ultrastructural observations – here on mouse and previously on chick (Yin et al., 2009) – show that, in mutant neural tube cells, the centrosome that will form the basal body of the cilium fails to dock with the apical cell membrane. A similar failure of centrosome positioning and/or docking is seen in cells lacking function in other genes encoding basal body proteins, including *Ofd1* (oral-facial-digital syndrome 1) (Singla et al., 2010) and *MKS1* (Meckel syndrome 1) (Dawe et al., 2007). Like cells of *talpid3*$^{-/-}$ mice, cells of *Ofd1*$^{-/-}$ (male mice) and *Mks1*$^{-/-}$ mouse mutants completely lack primary cilia. By contrast, loss of another centrosomal protein, RPGRIP1L (also known as FTM; which is responsible for Joubert syndrome type B and Meckel syndrome), results in fewer and/or malformed cilia (Vierkotten et al., 2007), and loss of BBS proteins (which are responsible for Bardet-Biedl syndrome) results in defects only in specialised cilia (for a review, see Goetz and Anderson, 2010).

Most features of the *talpid3*$^{-/-}$ mouse are similar to those of the *talpid*^{3} mutant chicken and attributable to abnormal Hh signalling (Table 1). In *talpid3*$^{-/-}$ mouse mutants, the neural tube is dorsalised and midline facial structures are lost. Both defects reflect loss of Gli2 activator activity. In mouse neural tube, graded Shh signalling mediates dorsoventral patterning, with high Gli2 activity specifying ventral neural tube progenitors (Wijgerde et al., 2002), whereas in mouse face, Shh is required for the formation of midline structures. Patients with loss-of-function mutations in *GLI2* also have mid-facial hypoplasia (Roessler et al., 2003). By contrast, *talpid*^{2} mutant chickens have an expanded facial midline, even though cells of this mutant have also been reported to lack cilia (Brugmann et al., 2010), resembling the hypertelorism seen in patients with *GLI3* haploinsufficiency (Biesecker, 2008) and with Bardet-Biedl syndrome (Beales et al., 1999).

Embryonic lethality characterises both mouse and chicken *talpid3* mutants but occurs earlier in mouse, although genetic background has an influence. The earlier demise of *talpid3*$^{-/-}$ mouse embryos might be due to vascularisation defects [as previously described in chicken *talpid*^{3} mutants (Davey et al., 2007)] impacting more severely on embryos with a placenta. *talpid3*$^{-/-}$ mouse embryos display randomised left/right asymmetry with respect to heart looping, consistent with the loss of nodal cilia (for a review, see Hirokawa et al., 2009). Preliminary observations suggest that *talpid*^{3} chicken mutant embryos have normal left/right asymmetry. The reasons for this are not clear. Further detailed analysis is on-going and will be reported elsewhere. It has recently been suggested that cilia do not play a role in establishing left/right asymmetry in chicken embryos as they do in other vertebrates, but rather asymmetrical cell movements lead to preferential left-sided *Shh* expression (Gros et al., 2009).

Other mouse mutants with homozygous mutations in genes encoding IFT components (*Kif3a* and *Ift88*), Hh signalling components (*Smo* and *Ptch1*), as well as centrosomal proteins required for ciliogenesis (*Ofd1*, males), exhibit a similar gross morphological phenotype to the *talpid3*$^{-/-}$ mutant mouse. In all cases, embryos survive until E9.5-10.5, turning is compromised, heart looping is randomised and there are neural tube defects and loss of facial midline structures (Goodrich et al., 1997; Takeda et al., 1999; Murcia et al., 2000; Zhang et al., 2001; Ferrante et al., 2006). *Mks1* mutant mice survive for longer (up until E18.5) even though the ciliogenesis defect is similar to that of *talpid3*$^{-/-}$ mice and they exhibit randomised heart looping and polydactyly (Weatherbee et al., 2009).

talpid3 CKO mouse limbs are remarkably similar to *talpid*^{3} chicken mutant limbs, i.e. they are polydactylous, short and syndactylous, even though effective loss of Talpid3 function, as witnessed by lack of cilia, is not abolished until E10.5, and then only in mesenchyme. This similarity suggests that Shh signalling is necessary only at later stages of limb development, fitting nicely with the phenotype of *Shh*$^{-/-}$ mouse embryonic limbs in which only structures distal to the elbow/knee are defective (Chiang et al., 2001). In *talpid3* CKO mouse forelimbs, up to nine morphologically indistinguishable digits develop, whereas in hind limbs polydactyly is reduced, with just a single extra digit, and digits arising in the posterior are more patterned. Both the increase in digit number and the absence of pattern can be ascribed to abnormal Shh signalling resulting from a lack of cilia, and the expression of Gli-regulated genes in early limb buds is consistent with this. Digit morphology in *talpid3* CKO limbs, particularly bifurcations, most closely resembles that in the limbs of mouse embryos that only express full-length Gli3 activator (Wang et al., 2007).

All forelimb digits and most digits in *talpid3* CKO mouse hind limbs lack one phalange. This brachydactyly, together with the shortening of long bones and accompanying growth plate changes and the failure to form subperiosteal bone, are seen in *Ihh* mouse mutants (St-Jacques et al., 1999). Calcified tissue is deposited in both *talpid3* CKO and *Ihh* mutant mouse long bones (St-Jacques et al., 1999); thus, maturation of chondrocytes occurs in *talpid3* CKO mouse long bones despite the inability to respond to Ihh signalling as evidenced by the lack of *Ptch1* expression. Calcified tissue has not been detected in *talpid*^{3} mutant chicken long bones (Macrae et al., 2010).

Similar patterning and skeletal defects to those in *talpid3* CKO limbs have been seen in *Prrx1* conditional limb knockouts of *Ift88*, *Kif3a* and *Ofd1*, including polydactyly and abnormal ossification (Haycraft et al., 2007; Bimonte et al., 2010). Even though *Ofd1* CKO mouse limbs end up with an almost identical skeletal phenotype to *talpid3* CKO mouse limb buds, Ofd1 protein levels are not reduced at E10.5 (Bimonte et al., 2010), whereas in *talpid3* CKO limb buds cilia are already absent by this stage. This suggests that timing cannot explain the difference in the extent of polydactyly between forelimb and hind limb. Limbs of patients with oral-facial-digital syndrome type 1, however, exhibit brachydactyly and syndactyly but not polydactyly [Online Mendelian Inheritance in Man (OMIM) ID #311200].

A striking difference between limbs of *talpid3* CKO mice and *talpid*^{3} chicken mutants is the extent of syndactyly. In the mouse, this only involves soft tissue, whereas in the chicken, especially wing, there is cartilaginous fusion. A possible reason for this difference is that *talpid3* function is only knocked out in mesenchyme in the mouse, whereas in the chicken it is absent in both mesenchyme and ectoderm. Reciprocal recombination of

ectoderm and mesenchyme from wild-type and *talpid*^{3} chicken leg buds shows that the limb phenotype is determined by mesenchyme (Ede and Shamslahidjani, 1983). This finding suggests that the wild-type nature of the ectoderm in *talpid3* CKO limb buds is not the reason for the differences in syndactyly. Formation of digit condensations and intervening interdigital spaces is delayed and irregular in *talpid3* CKO mouse limbs, whereas in *talpid*^{3} chicken mutant limbs no interdigital spaces expressing *Raldh2* are seen at a stage when this process is complete in wild type, correlating with extensive digital fusion. Interestingly, we showed sometime ago that implanting a bead soaked in retinoic acid or grafting a polarising region to wing buds of *talpid*^{3} chicken mutant embryos could, to some extent, rescue syndactyly and result in digit separation (Francis-West et al., 1995).

Both mouse and chicken *talpid*^{3} mutant limb buds have a dramatically altered shape, being broader and shorter than wild-type limb buds. Donald Ede (Ede, 1971) suggested that the shape of the chicken mutant wing bud could be due to changes in cell proliferation or in the ability of cells to polarise. We found that *talpid3*$^{-/-}$ mouse cells take longer to migrate into a scratch and have less directionality than wild-type cells. This fits with recent work on cells from OPRK (*Ift88*^{Tg737Rpw}) mice suggesting that primary cilia co-ordinate directional cell migration and chemotaxis (Schneider et al., 2010). The changed behaviour of *talpid3*$^{-/-}$ mutant cells is also intriguing in view of the suggestion that directional cell movement determines limb shape (Wyngaarden et al., 2010); thus, *talpid3* CKO limbs could be a useful model to study morphogenesis.

Acknowledgements

We thank Alan Prescott, John James and Ursula Potter for electron microscopy; Louise Anderson and annex staff for their help; and Philip Beales, Malcolm Logan, Kate Nobes and Dominic Norris for discussions. We are grateful for support from the BBSRC (F.B., M.W., M.G.D.), MRC (F.B., N.A.) and The Royal Society (C.T.). Deposited in PMC for release after 6 months.

Competing interests statement

The authors declare no competing financial interests.

Supplementary material

Supplementary material for this article is available at
http://dev.biologists.org/lookup/suppl/doi:10.1242/dev.063602/-/DC1

References

Abbott, U. K., Taylor, L. W. and Abplanalp, H. (1959). A second *talpid*-like mutation in the fowl. *Poult. Sci.* **38**, 1185.

Akiyama, H., Chaboisssier, M. C., Martin, J. F., Schedl, A. and de Crombrugghe, B. (2002). The transcription factor Sox9 has essential roles in successive steps of the chondrocyte differentiation pathway and is required for expression of Sox5 and Sox6. *Genes Dev.* **16**, 2813-2828.

Baker, K. and Beales, P. L. (2009). Making sense of cilia in disease: the human ciliopathies. *Am. J. Med. Genet. C Semin. Med. Genet.* **151C**, 281-295.

Beales, P. L., Elcioglu, N., Woolf, A. S., Parker, D. and Flinter, F. A. (1999). New criteria for improved diagnosis of Bardet-Biedl syndrome: results of a population survey. *J. Med. Genet.* **36**, 437-446.

Biesecker, L. G. (2008). The Greig cephalopolysyndactyly syndrome. *Orphanet. J. Rare Dis.* **3**, 10.

Bimonte, S., De Angelis, A., Quagliata, L., Giusti, F., Tammaro, R., Dallai, R., Ascenzi, M. G., Diez-Roux, G. and Franco, B. (2010). Ofd1 is required in limb bud patterning and endochondral bone development. *Dev. Biol.* **349**, 179-191.

Brennan, J., Lu, C. C., Norris, D. P., Rodriguez, T. A., Beddington, R. S. and Robertson, E. J. (2001). Nodal signalling in the epiblast patterns the early mouse embryo. *Nature* **411**, 965-969.

Brugmann, S. A., Allen, N. C., James, A. W., Mekonnen, Z., Madan, E. and Helms, J. A. (2010). A primary cilia-dependent etiology for midline facial disorders. *Hum. Mol. Genet.* **19**, 1577-1592.

Buxton, P., Davey, M. G., Paton, I. R., Morrice, D. R., Francis-West, P. H., Burt, D. W. and Tickle, C. (2004). Craniofacial development in the talpid3 chicken mutant. *Differentiation* **72**, 348-362.

Chiang, C., Littingtung, Y., Harris, M. P., Simandl, B. K., Li, Y., Beachy, P. A. and Fallon, J. F. (2001). Manifestation of the limb prepattern: limb development in absence of sonic hedgehog function. *Dev. Biol.* **236**, 421-435.

Cole, R. K. (1942). The *talpid* lethal in the domestic foul. *J. Hered.* **33**, 82-86.

Davey, M. G., Paton, I. R., Yin, Y., Schmidt, M., Bangs, F. K., Morrice, D. R., Smith, T. G., Buxton, P., Stamataki, D., Tanaka, M. et al. (2006). The chicken talpid3 gene encodes a novel protein essential for Hedgehog signaling. *Genes Dev.* **20**, 1365-1377.

Davey, M. G., James, J., Paton, I. R., Burt, D. W. and Tickle, C. (2007). Analysis of talpid3 and wild-type chicken embryos reveals roles for Hedgehog signalling in development of the limb bud vasculature. *Dev. Biol.* **301**, 155-165.

Dawe, H. R., Smith, U. M., Cullinane, A. R., Gerrelli, D., Cox, P., Badano, J. L., Blair-Reid, S., Sriram, N., Katsanis, N., Attie-Bitach, T. et al. (2007). The Meckel-Gruber Syndrome proteins MKS1 and meckelin interact and are required for primary cilium formation. *Hum. Mol. Genet.* **16**, 173-186.

Ede, D. A. (1971). Control of form and pattern in the vertebrate limb. *Symp. Soc. Exp. Biol.* **25**, 235-254.

Ede, D. A. and Kelly, W. A. (1964a). Developmental abnormalities in the head region of the talpid mutant of the fowl. *J. Embryol. Exp. Morphol.* **12**, 161-182.

Ede, D. A. and Kelly, W. A. (1964b). Developmental abnormalities in the trunk and limbs of the fowl. *J. Embryol. Exp. Morphol.* **12**, 339-356.

Ede, D. A. and Agerbak, G. S. (1968). Cell adhesion and movement in relation to the developing limb pattern in normal and talpid mutant chick embryos. *J. Embryol. Exp. Morphol.* **20**, 81-100.

Ede, D. A. and Shamslahidjani, M. (1983). Ectoderm/mesoderm recombination, dissociation and cell aggregation studies in normal and talpid mutant avian embryos. *Prog. Clin. Biol. Res.* **110**, 45-55.

Ferrante, M. I., Zullo, A., Barra, A., Bimonte, S., Messaddeq, N., Studer, M., Dollé, P. and Franco, B. (2006). Oral-facial-digital type I protein is required for primary cilia formation and left-right axis specification. *Nat. Genet.* **38**, 112-117.

Fisher, M. E., Clelland, A. K., Bain, A., Baldock, R. A., Murphy, P., Downie, H., Tickle, C. R., Davidson, D. R. and Buckland, R. A. (2008). Integrating technologies for comparing 3D gene expression domains in the developing chick limb. *Dev. Biol.* **317**, 13-23.

Francis-West, P. H., Robertson, K. E., Ede, D. A., Rodriguez, C., Izpisúa-Belmonte, J. C., Houston, B., Burt, D. W., Gribbin, C., Brickell, P. M. and Tickle, C. (1995). Expression of genes encoding bone morphogenetic proteins and sonic hedgehog in talpid (ta3) limb buds: their relationships in the signalling cascade involved in limb patterning. *Dev. Dyn.* **203**, 187-197.

Goetz, S. C. and Anderson, K. V. (2010). The primary cilium: a signalling centre during vertebrate development. *Nat. Rev. Genet.* **11**, 331-344.

Goodrich, L. V., Milenković, L., Higgins, K. M. and Scott, M. P. (1997). Altered neural cell fates and medulloblastoma in mouse patched mutants. *Science* **277**, 1109-1113.

Gros, J., Feistel, K., Viebahn, C., Blum, M. and Tabin, C. J. (2009). Cell movements at Hensen's node establish left/right asymmetric gene expression in the chick. *Science* **324**, 941-944.

Haycraft, C. J., Zhang, Q., Song, B., Jackson, W. S., Detloff, P. J., Serra, R. and Yoder, B. K. (2007). Intraflagellar transport is essential for endochondral bone formation. *Development* **134**, 307-316.

Hirokawa, N., Tanaka, Y. and Okada, Y. (2009). Left-right determination: involvement of molecular motor KIF3, cilia, and nodal flow. *Cold Spring Harb. Perspect. Biol.* **1**, a000802.

Hogan, B. and Lacy, E. (1994). *Manipulating the Mouse Embryo: a Laboratory Manual*. Plainview, NY: Cold Spring Harbor Laboratory Press.

Izpisúa-Belmonte, J. C., Ede, D. A., Tickle, C. and Duboule, D. (1992). The mis-expression of posterior Hox-4 genes in talpid (ta3) mutant wings correlates with the absence of anteroposterior polarity. *Development* **114**, 959-963.

Kuss, P., Villavicencio-Lorini, P., Witte, F., Klose, J., Albrecht, A. N., Seeman, P., Hecht, J. and Mundlos, S. (2009). Mutant Hoxd13 induces extra digits in a mouse model of synpolydactyly directly and by decreasing retinoic acid synthesis. *J. Clin. Invest.* **119**, 146-156.

Lewis, K. E., Drossopoulou, G., Paton, I. R., Morrice, D. R., Robertson, K. E., Burt, D. W., Ingham, P. W. and Tickle, C. (1999). Expression of ptc and gli genes in talpid3 suggests bifurcation in Shh pathway. *Development* **126**, 2397-2407.

Logan, M., Martin, J. F., Nagy, A., Lobe, C., Olson, E. N. and Tabin, C. J. (2002). Expression of Cre recombinase in the developing mouse limb bud driven by a Prxl enhancer. *Genesis* **33**, 77-80.

Macrae, V. E., Davey, M. G., McTeir, L., Narisawa, S., Yadav, M. C., Millan, J. L. and Farquharson, C. (2010). Inhibition of PHOSPHO1 activity results in impaired skeletal mineralization during limb development of the chick. *Bone* **46**, 1146-1155.

Matise, M. P., Epstein, D. J., Park, H. L., Platt, K. A. and Joyner, A. L. (1998). Gli2 is required for induction of floor plate and adjacent cells, but not most ventral neurons in the mouse central nervous system. *Development* **125**, 2759-2770.

Moorman, A. F., Houweling, A. C., de Boer, P. A. and Christoffels, V. M. (2001). Sensitive nonradioactive detection of mRNA in tissue sections: novel

application of the whole-mount in situ hybridization protocol. *J. Histochem. Cytochem.* **49**, 1-8.
Murcia, N. S., Richards, W. G., Yoder, B. K., Mucenski, M. L., Dunlap, J. R. and Woychik, R. P. (2000). The Oak Ridge Polycystic Kidney (orpk) disease gene is required for left-right axis determination. *Development* **127**, 2347-2355.
Niederreither, K., McCaffery, P., Dräger, U. C., Chambon, P. and Dollé, P. (1997). Restricted expression and retinoic acid-induced downregulation of the retinaldehyde dehydrogenase type 2 (RALDH-2) gene during mouse development. *Mech. Dev.* **62**, 67-78.
Riddle, R. D., Johnson, R. L., Laufer, E. and Tabin, C. (1993). Sonic hedgehog mediates the polarizing activity of the ZPA. *Cell* **75**, 1401-1416.
Roessler, E., Du, Y. Z., Mullor, J. L., Casas, E., Allen, W. P., Gillessen-Kaesbach, G., Roeder, E. R., Ming, J. E., Ruiz i Altaba, A. and Muenke, M. (2003). Loss-of-function mutations in the human GLI2 gene are associated with pituitary anomalies and holoprosencephaly-like features. *Proc. Natl. Acad. Sci. USA* **100**, 13424-13429.
Saunders, J. W. and Gasseling, M. T. (1968). Ectodermal-mesenchymal interactions in the origin of limb symmetry. In *Epithelial-mesenchymal Interactions* (ed. R. Fleischmeyer and R. E. Billingham), pp. 78-97. Baltimore: Williams & Wilkins.
Schmidt, K., Hughes, C., Chudek, J. A., Goodyear, S. R., Aspden, R. M., Talbot, R., Gundersen, T. E., Blomhoff, R., Henderson, C., Wolf, C. R. et al. (2009). Cholesterol metabolism: the main pathway acting downstream of cytochrome P450 oxidoreductase in skeletal development of the limb. *Mol. Cell. Biol.* **29**, 2716-2729.
Schneider, L., Cammer, M., Lehman, J., Nielsen, S. K., Guerra, C. F., Veland, I. R., Stock, C., Hoffmann, E. K., Yoder, B. K., Schwab, A. et al. (2010). Directional cell migration and chemotaxis in wound healing response to PDGF-AA are coordinated by the primary cilium in fibroblasts. *Cell. Physiol. Biochem.* **25**, 279-292.
Singla, V., Romaguera-Ros, M., Garcia-Verdugo, J. M. and Reiter, J. F. (2010). Ofd1, a human disease gene, regulates the length and distal structure of centrioles. *Dev. Cell* **18**, 410-424.
St-Jacques, B., Hammerschmidt, M. and McMahon, A. P. (1999). Indian hedgehog signaling regulates proliferation and differentiation of chondrocytes and is essential for bone formation. *Genes Dev.* **13**, 2072-2086.
Storm, E. E. and Kingsley, D. M. (1999). GDF5 coordinates bone and joint formation during digit development. *Dev. Biol.* **209**,11-27.
Takeda, S., Yonekawa, Y., Tanaka, Y., Okada, Y., Nonaka, S. and Hirokawa, N. (1999). Left-right asymmetry and kinesin superfamily protein KIF3A: new insights in determination of laterality and mesoderm induction by kif3A–/– mice analysis. *J. Cell Biol.* **145**, 825-836.
Tickle, C. (2006). Making digit patterns in the vertebrate limb. *Nat. Rev. Mol. Cell Biol.* **7**, 45-53.
Tiecke, E., Turner, R., Sanz-Ezquerro, J. J., Warner, A. and Tickle, C. (2007). Manipulations of PKA in chick limb development reveal roles in digit patterning including a positive role in Sonic Hedgehog signaling. *Dev. Biol.* **305**, 312-324.
Towers, M., Mahood, R., Yin, Y. and Tickle, C. (2008). Integration of growth and specification in chick wing digit-patterning. *Nature* **452**, 882-886.
Vierkotten, J., Dildrop, R., Peters, T., Wang, B. and Rüther, U. (2007). Ftm is a novel basal body protein of cilia involved in Shh signalling. *Development* **134**, 2569-2577.
Vortkamp, A., Franz, T., Gessler, M. and Grzeschik, K. H. (1992). Deletion of GLI3 supports the homology of the human Greig cephalopolysyndactyly syndrome (GCPS) and the mouse mutant extra toes (Xt). *Mamm. Genome* **3**, 461-463.
Wang, C., Rüther, U. and Wang, B. (2007). The Shh-independent activator function of the full-length Gli3 protein and its role in vertebrate limb digit patterning. *Dev. Biol.* **305**, 460-469.
Weatherbee, S. D., Niswander, L. A. and Anderson, K. V. (2009). A mouse model for Meckel syndrome reveals Mks1 is required for ciliogenesis and Hedgehog signaling. *Hum. Mol. Genet.* **18**, 4565-4575.
Wijgerde, M., McMahon, J. A., Rule, M. and McMahon, A. P. (2002). A direct requirement for Hedgehog signaling for normal specification of all ventral progenitor domains in the presumptive mammalian spinal cord. *Genes Dev.* **16**, 2849-2864.
Wilkinson, D. G. and Nieto, M. A. (1993). Detection of messenger RNA by in situ hybridization to tissue sections and whole mounts. *Methods Enzymol.* **225**, 361-373.
Wyngaarden, L. A., Vogeli, K. M., Ciruna, B. G., Wells, M., Hadjantonakis, A. K. and Hopyan, S. (2010). Oriented cell motility and division underlie early limb bud morphogenesis. *Development* **137**, 2551-2558.
Yang, Y., Drossopoulou, G., Chuang, P. T., Duprez, D., Marti, E., Bumcrot, D., Vargesson, N., Clarke, J., Niswander, L., McMahon, A. et al. (1997). Relationship between dose, distance and time in Sonic Hedgehog-mediated regulation of anteroposterior polarity in the chick limb. *Development* **124**, 4393-4404.
Yin, Y., Bangs, F., Paton, I. R., Prescott, A., James, J., Davey, M. G., Whitley, P., Genikhovich, G., Technau, U., Burt, D. W. et al. (2009). The Talpid3 gene (KIAA0586) encodes a centrosomal protein that is essential for primary cilia formation. *Development* **136**, 655-664.
Zhang, X. M., Ramalho-Santos, M. and McMahon, A. P. (2001). Smoothened mutants reveal redundant roles for Shh and Ihh signaling including regulation of L/R symmetry by the mouse node. *Cell* **106**, 781-792.
Zhu, J., Nakamura, E., Nguyen, M. T., Bao, X., Akiyama, H. and Mackem, S. (2008). Uncoupling Sonic hedgehog control of pattern and expansion of the developing limb bud. *Dev. Cell* **14**, 624-632.